ACS Sustainable Chemistry & Engineering

Letter

pubs.acs.org/journal/ascecg

Eggshell Membrane-Derived Polysulfide Absorbents for Highly Stable and Reversible Lithium−Sulfur Cells

Sheng-Heng Chung and Arumugam Manthiram*

Materials Science and Engineering Program and Texas Materials Institute, The University of Texas at Austin, Austin, Texas 78712, United States

Supporting Information

ABSTRACT: The carbonized eggshell membrane (CEM) powder with abundant micropores and high porosity is embedded within conventional sulfur cathodes (CEM-S cathodes) as a polysulfide (PS) absorbent for lithium−sulfur batteries. The CEM PS absorbent effectively limits the irreversible active material loss from CEM-S cathodes and prevents the formation of severe inactive agglomerations on the surface of the cathode during cycling. In addition to trapping the migrating PSs, the conductive and porous CEM facilitates efficient electron transport and electrolyte immersion, which ensures successive reactivation and reutilization of the trapped active material. As a result, the CEM-S cathodes with a reasonable sulfur content of 60 wt % exhibit a high capacity retention rate of 85% and a low capacity fade rate of 0.10% per cycle for 150 cycles. Such superior cycle stability suggests that natural starting materials with unique porous structures can be utilized to manufacture high-performance cell components for Li−S cells.

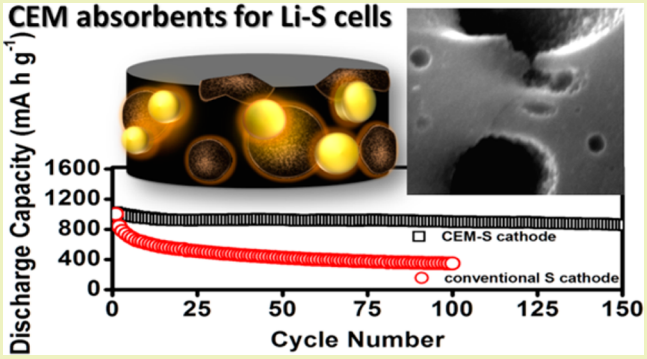

KEYWORDS: *Lithium−sulfur batteries, Eggshell membrane, Polysulfide absorbent, Electrochemistry, Natural products*

INTRODUCTION

The high energy density rechargeable lithium−sulfur (Li−S) battery is an attractive power source for electric vehicles and grid storage. During cell discharge, the cathodic reaction of a Li−S battery involves a reduction reaction of the S cathode: $S + 2Li^+ + 2e^- \rightarrow Li_2S$. The active S material first reduces to polysulfides (PSs, Li_2S_x, $4 < x \leq 8$), and then the PSs convert to the end-discharge products (Li_2S_2/Li_2S) with a shortening of the S chain length. The anodic reaction is an oxidation reaction of the Li-metal anode: $2Li \rightarrow 2Li^+ + 2e^-$. The overall discharge reaction is $2Li + S \rightarrow Li_2S$.[1] As a result, the environmentally benign sulfur has a high theoretical capacity of 1672 mA h g^{-1}, enabling packed cells with two to three times higher energy densities than currently used Li-ion batteries.[1,2] Over the years, nanocomposites, polymers, and novel cell configurations have been designed to enhance sulfur utilization.[3−7] Composite cathodes[3,4,8−11] and new cell designs[5,12−16] increase the discharge capacity by wiring the insulating sulfur and introducing electron pathways for the low-conductive sulfur cathodes. Porous carbon substrates further enhance the electrochemical reversibility and provide long-term stability by physically and chemically trapping the diffusing PSs.[8−18] The PSs that form at intermediate discharge/charge states are highly soluble in the liquid electrolyte currently used in Li−S cells.[5,6] The dissolved PSs easily diffuse through the separator, react with the Li-metal anode, and shuttle between the anode and cathode. The severe PS diffusion causes rapid capacity fade, poor electrochemical efficiency, and low active material reutilization.[5−7]

To mitigate the PS diffusion, the on-site adsorption/absorption method that directly traps the PSs within the cathode is a promising approach. A few oxide nanoparticle[19−22] or porous substrates[23−25] have been mixed within the cathode as the "PS adsorbent/absorbent" for immobilizing the PSs and enhancing cell stability. Recently, various natural raw materials have been applied in different cell systems, such as the carbonized eggshell membrane electrodes in Li/dissolved polysulfide cells,[26] carbonized leaf interlayer in Li−S cells,[27] carbohydrate-derived nanocomposites in Li−S cells,[28] and cellulose composite separator in Li-ion cells.[29] Thus, it is reasonable to expect that natural starting materials are possible to replace engineered starting materials and achieve the same engineering goals.

In this Letter, we present the use of carbonized eggshell membranes (CEMs) in sulfur cathodes as a PS absorbent. After carbonization at 800 °C in an inert argon atmosphere, the CEM absorbent has abundant micropores for absorbing the migrating PSs, effectively mitigating the severe PS diffusion.[8,10] After absorbing the PSs, the conductive CEM provides fast electron transport, ensuring the continuous reactivation and reutilization

Received: July 11, 2014
Revised: September 14, 2014
Published: September 15, 2014

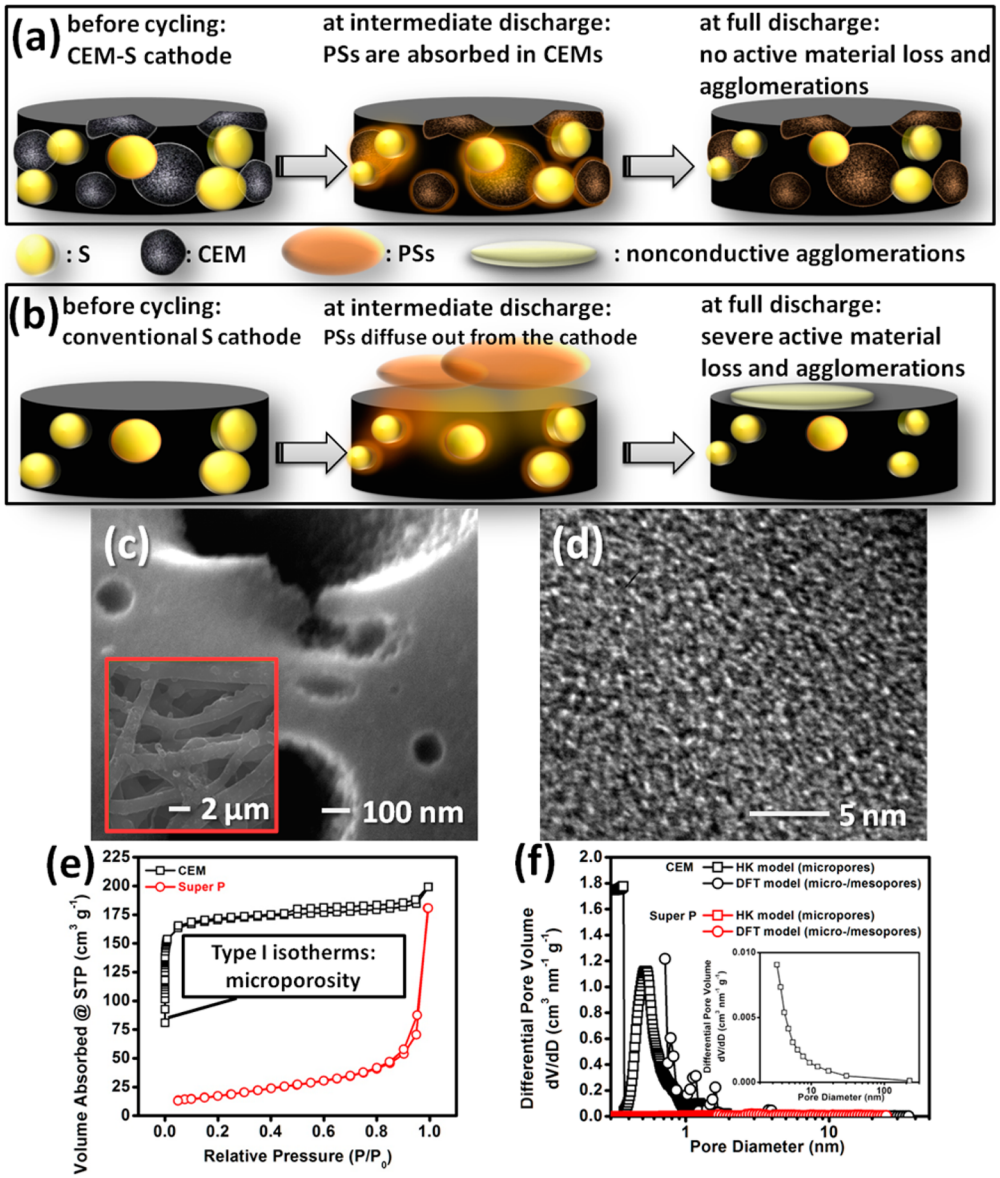

Figure 1. Schematics of (a) CEM-S cathode and (b) conventional S cathode. Microstructural analysis of CEMs: (c) SEM observation (inset is CEM sheet), (d) TEM observation, (e) Brunner–Emmett–Teller (BET) isotherms, and (f) pore-size distributions with Horvath–Kawazoe (HK) and density functional theory (DFT) models (inset is Barrett–Joyer–Halenda (BJH) model).

of the trapped active material. Therefore, the CEM-S cathode with 10 wt % CEM absorbent offers a high reversible capacity of 860 mA h g^{-1} with an excellent capacity retention rate of 85% and a low capacity fade rate of 0.10% per cycle for 150 cycles.

EXPERIMENTAL SECTION

CEM and CEM-S cathode preparation. The eggshell was washed with deionized (DI) water, and the $CaCO_3$ shell was etched away in 1 M HCl for 2 h. After rinsing with DI water, the remaining organic eggshell membrane was immersed into a 40 wt % sucrose solution (sucrose, Fisher Scientific), followed by precarbonization at 180 °C for 12 h. The precarbonized CEM was subsequently carbonized at 800 °C for 12 h with a heating rate of 1 °C min^{-1} in a tube furnace in argon atmosphere. After carbonization, the CEM sheet was ground into micron-sized CEM powders. The CEM-S cathode contained 60 wt % precipitated sulfur, 10 wt % CEM powder, 15 wt % Super P carbon (TIMCAL), and 15 wt % polyvinylidene fluoride (PVDF, Kureha) binder. The sulfur content and loading in CEM-S cathodes are, respectively, 60 wt % and ~1.3 mg cm^{-2}.

RESULTS AND DISCUSSION

Porous CEMs are expected to absorb the PSs within the cathode region via their natural micropores and high porosity,[23−25] as illustrated in Figure 1a and b. During cell discharge, the PSs produced are absorbed by the porous CEMs, suppressing the severe PS diffusion. At full discharge, the absorbed PSs reduce to Li_2S_2/Li_2S, which are tightly held and surrounded by the conductive CEM and Super P carbon. This avoids the formation of nonconductive precipitation on the exterior surface of the electrodes and improves the connection between the active material and conductive additives.[12,15] As a reference, the Super P is a commercial conductive carbon commonly used in cathode preparation in Li–S and Li-ion batteries. During cell charge, the conductive and porous CEM provides efficient electron/charge transport and electrolyte

dx.doi.org/10.1021/sc500452j | ACS Sustainable Chem. Eng. 2014, 2, 2248−2252

immersion, ensuring the reversible conversion reaction from Li_2S_2/Li_2S to Li_2S_8/S_8.[15,23]

After carbonization, the organic eggshell membrane converts into a carbon thin film with a uniform fibrous network structure, as shown in the scanning electron microscopy (SEM) images and the corresponding elemental mapping results (Figure S1, Supporting Information). Figure S2 of the Supporting Information indicates that the ground CEM powder mainly consists of carbon. The Raman spectrum of CEMs shows two carbon peaks at ~1349 cm^{-1} (disorder-induced D band) and ~1590 cm^{-1} (graphitic G band). The intensity of the G band to the D band indicates that the CEM is a partially graphitized carbonaceous material, which is known as an appealing electrode material because of its high conductivity.[30] In Figure 1c and d, the SEM and transmission electron microscopy (TEM) images depict that CEMs possess abundant micropores intrinsically composited on their meso-/macroporous structure. The micropore is the major factor for absorbing the PSs before they escape out of the cathode region.[8,10,26] The meso-/macropore functions are the electrolyte pathways for (i) channeling the liquid electrolyte containing the dissolved PSs to the micropores and (ii) transporting charges and electrolyte for reactivating the absorbed active material.[10,15,23−25] After immobilizing the diffusing PSs, the porous CEM tolerates the volume changes from the trapped active material during repeated cycling, ensuring intimate connection between the active material and conductive carbon. The natural micropores and high porosity of CEMs are assessed by nitrogen adsorption−desorption isotherms (Figure 1e) and pore-size distribution curves (Figure 1f). The CEM has a high surface area of 487 $m^2\ g^{-1}$ with a micropore area of 315 $m^2\ g^{-1}$ and a total pore volume of 0.31 $cm^3\ g^{-1}$ with a micropore volume of 0.25 $cm^3\ g^{-1}$. The IUPAC type I isotherms[31] and a high fraction of micropores in the pore-size distribution curves demonstrate high microporosity in CEMs. On the other hand, the Super P conductive carbon shows a relatively low surface area (63 $m^2\ g^{-1}$) with no micropores.

Figure 2a shows the cyclic voltammetry (CV) curves of the CEM-S cathode at a scan rate of 0.05 mV s^{-1} during the initial 20 cycles. During cell discharge, the CV curves display the typical two-step reduction reactions. The cathodic peak I starting at ~2.4 V indicates the reduction reaction from S_8 to soluble PSs. The cathodic peak II starting at ~2.1 V corresponds to subsequent reduction reaction from soluble PSs to the end-discharge products (Li_2S_2/Li_2S).[32−34] During cell charge, the two overlapping anodic peaks III and IV represent the continuous oxidization reactions from Li_2S_2/Li_2S to PSs and from PSs to Li_2S_8/S_8.[3,7,18] The overlapping anodic peaks depict that the S_8^{2-} intermediate with a facile oxidation kinetic may be one of the end-charge products.[3] During repeated cycling, the CV curves exhibit overlapping cathodic and anodic peaks, indicating good electrochemical stabilization of the CEM-S cathode. Figure 2b presents the discharge/charge voltage profiles of the cell utilizing the CEM-S cathode at a C/10 rate for 150 cycles. The cycling rate (C/10) is based on the mass and theoretical capacity of sulfur (1C = 1672 mA g^{-1}). During long-term cycling (150 cycles), the well-retained upper-discharge plateaus (signified as I) demonstrate that the migrating PSs are absorbed into the CEM absorbent, and severe active material loss has not occurred.[32,34] The almost complete lower-discharge plateaus (signified as II) attest to the excellent reversibility of the CEM-S cathode. During cell

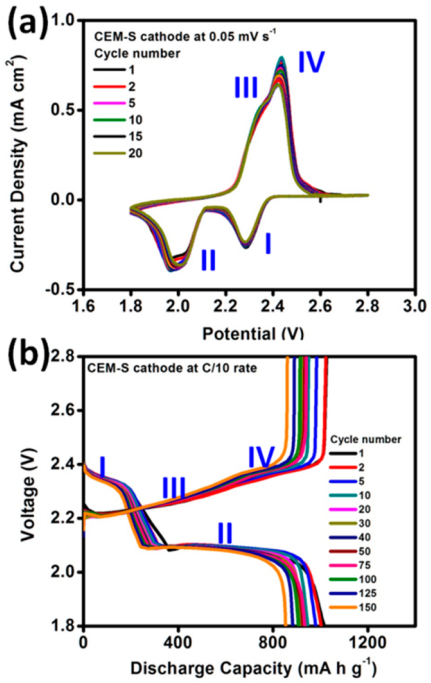

Figure 2. Electrochemical measurements of Li−S cells employing the CEM-S cathode: (a) cyclic voltammograms at a 0.05 mV s^{-1} scanning rate and (b) discharge/charge curves at a C/10 rate.

charge, the vertical voltage rise from 2.4 to 2.8 V indicates a complete charge reaction.[34,35] These improvements were not observed with the conventional S cathode (sulfur cathodes without CEMs), as shown in Figure S3 of the Supporting Information.

The electrochemical impedance spectroscopy (EIS) data of the CEM-S cathode (Figure S4, Supporting Information) exhibit a stable cathode resistance of as low as 40−50 Ohm for 30 cycles, which is not seen with the conventional S cathode. The increase in resistance observed in the conventional S cathode may result from the redeposition of the diffusing PSs that forms nonconductive agglomerations on the surface of conventional S cathodes during cycling (Figure S5, Supporting Information).[23−25] The nonconductive agglomeration is believed to be Li_2S/Li_2S_2 mixtures, as reported in the Li−S literature.[3,36] On the other hand, a comparison of the CEM-S cathode before and after cycling shows no obvious morphological changes (Figure S6, Supporting Information). The cycled CEM-S cathode displays the elemental sulfur signals uniformly distributed in the carbon matrix. These indicate no apparent active material loss from the cathode and no inactive agglomerates on the cathode.

Figure 3a shows the comparison of the cyclability between the CEM-S cathodes and the conventional S cathode. The initial discharge capacities (Q_1) of the CEM-S cathode and the conventional S cathode are, respectively, 1016 and 1000 mA h g^{-1}. After the first cycle, the CEM-S cathode exhibits a high reversible capacity of 1002 mA h g^{-1} in the second cycle (Q_2) with excellent capacity retention (Q_2/Q_1) of 99%. However, the conventional S cathode shows severe capacity fade from 1000 to 837 mA h g^{-1} (Q_2/Q_1 = 84%) after one cycle. The high reversibility of the CEM-S cathode indicates that the PSs are absorbed by CEMs. Thus, the cycled CEM absorbents display distinguishable elemental sulfur signals in CEM absorbents, as shown in Figure 3b and Figure S7 of the Supporting

dx.doi.org/10.1021/sc500452j | ACS Sustainable Chem. Eng. 2014, 2, 2248−2252

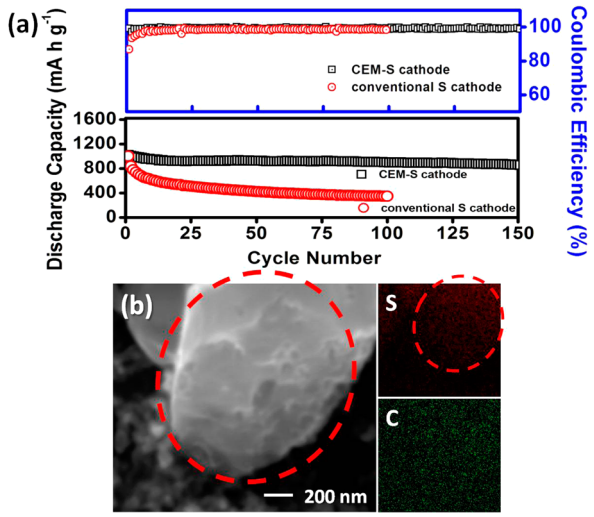

Figure 3. (a) Long-term cyclability of the Li−S cells employing the CEM-S cathode and conventional S cathode. (b) SEM observation and elemental mapping of the cycled CEM absorbent.

Information. This confirms that the active material is stabilized within the CEM-S cathode. As a result, the CEM absorbent ensures cells to accomplish stable cyclability over 150 cycles with a reversible capacity of 860 mA h g^{-1} and an average Coulombic efficiency above 98%, indicating high reversibility and minimal shuttle effect. The corresponding capacity retention (Q_{150}/Q_1) after 150 cycles is 85% (Figure S8, Supporting Information), and the capacity fade rate is only 0.10% per cycle. Such superior cycle stability results from the use of CEM absorbents within the cathode for efficiently absorbing the migrating PSs. A comparative analysis with other PS adsorbent/absorbent derived from engineering raw materials indicates that the CEM absorbent offers excellent long-term cyclability for Li−S batteries (Table S1,Supporting Information).[19−25]

CONCLUSION

In summary, the CEM derived from a sustainable natural eggshell membrane with a unique porous structure has been evidenced as a high-performance PS absorbent for improving the cycle stability of Li−S batteries. The CEM absorbent with inherent microporous absorption sites prevents severe active material loss and redeposition of nonconductive agglomerations on the surface of CEM-S cathodes during cycling. Therefore, the CEM-S cathode with a reasonable sulfur content of 60 wt % provides Li−S cells with a high reversible capacity of 860 mA h g^{-1} and a low capacity fade rate of 0.10% per cycle for 150 cycles.

ASSOCIATED CONTENT

Supporting Information

Experimental details, summary of the performance data of the Li−S batteries with adsorbents/absorbents, and additional electrochemical and microstructural analyses. This material is available free of charge via the Internet at http://pubs.acs.org.

AUTHOR INFORMATION

Corresponding Author

*Phone: (512) 471-1791. Fax: (512) 471-7681. E-mail: rmanth@mail.utexas.edu.

Author Contributions

The manuscript was written through contributions of all authors. All authors have given approval to the final version of the manuscript.

Notes

The authors declare no competing financial interest.

ACKNOWLEDGMENTS

This work was supported by the U.S. Department of Energy, Office of Basic Energy Sciences, Division of Materials Sciences and Engineering under Award DE-SC0005397.

REFERENCES

(1) Bruce, P. G.; Freunberger, S. A.; Hardwick, L. J.; Tarascon, J.-M. Li−O_2 and Li−S batteries with high energy storage. *Nat. Mater.* **2012**, *11*, 19−29.
(2) Rauh, R. D.; Abraham, K. M.; Pearson, G. F.; Surprenant, J. K.; Brummer, S. B. A lithium/dissolved sulfur battery with an organic electrolyte. *J. Electrochem. Soc.* **1979**, *126*, 523−527.
(3) Ji, X.; Nazar, L. Advances in Li−S batteries. *J. Mater. Chem.* **2010**, *20*, 9821−9826.
(4) Ji, X.; Lee, K.; Nazar, L. A highly ordered nanostructured carbon-sulphur cathode for lithium−sulphur batteries. *Nat. Mater.* **2009**, *8*, 500−506.
(5) Manthiram, A.; Fu, Y.; Su, Y.-S. Challenges and prospects of lithium−sulfur batteries. *Acc. Chem. Res.* **2012**, *46*, 1125−1134.
(6) Evers, S.; Nazar, L. F. New approaches for high energy density lithium−sulfur battery cathodes. *Acc. Chem. Res.* **2013**, *46*, 1135−1143.
(7) Yin, Y.-X.; Xin, S.; Guo, Y.-G.; Wan, L.-J. Lithium−sulfur batteries: Electrochemistry, materials, and prospects. *Angew. Chem., Int. Ed.* **2013**, *52*, 13186−13200.
(8) Zhang, B.; Qin, X.; Li, G. R.; Gao, X. P. Enhancement of long stability of sulfur cathode by encapsulating sulfur into micropores of carbon spheres. *Energy Environ. Sci.* **2010**, *3*, 1531−1537.
(9) Sun, X.-G.; Wang, X.; Mayes, R. T.; Dai, S. Lithium−sulfur batteries based on nitrogen-doped carbon and an ionic-liquid electrolyte. *ChemSusChem* **2012**, *5*, 2079−2085.
(10) Lee, J. T.; Zhao, Y.; Thieme, S.; Kim, H.; Oschatz, M.; Borchardt, L.; Magasinski, A.; Cho, W.-I.; Kaskel, S.; Yushin, G. Sulfur-infiltrated micro- and mesoporous silicon carbide-derived carbon cathode for high-performance lithium sulfur batteries. *Adv. Mater.* **2013**, *25*, 4573−4579.
(11) Wang, L.; Zhao, Y.; Thomas, M. L.; Byon, H. R. In situ synthesis of bipyramidal sulfur with 3D carbon nanotube framework for lithium−sulfur batteries. *Adv. Funct. Mater.* **2014**, *24*, 2248−2252.
(12) Elazari, R.; Salitra, G.; Garsuch, A.; Panchenko, A.; Aurbach, D. Sulfur-impregnated activated carbon fiber cloth as a binder-free cathode for rechargeable Li−S batteries. *Adv. Mater.* **2011**, *23*, 5641−5644.
(13) Barchasz, C.; Mesguich, F.; Dijon, J.; Leprêtre, J.-C.; Patoux, S.; Alloin, F. Novel positive electrode architecture for rechargeable lithium/sulfur batteries. *J. Power Sources* **2102**, *211*, 19−26.
(14) Moon, S.; Jung, Y. H.; Jung, W. K.; Jung, D. S.; Choi, J. W.; Kim, D. K. Encapsulated monoclinic sulfur for stable cycling of Li−S rechargeable batteries. *Adv. Mater.* **2013**, *25*, 6547−6553.
(15) Chung, S.-H.; Manthiram, A. Low-cost, porous carbon current collector with high sulfur loading for lithium-sulfur batteries. *Electrochem. Commun.* **2014**, *38*, 91−95.
(16) Zhou, G.; Pei, S.; Li, L.; Wang, D.-W.; Wang, S.; Huang, K.; Yin, L.-C.; Li, F.; Cheng, H.-M. A graphene-pure-sulfur sandwich structure for ultrafast, long-life lithium−sulfur batteries. *Adv. Mater.* **2014**, *26*, 625−631.
(17) Schuster, J.; He, G.; Mandlmeier, B.; Yim, T.; Lee, K.; Bein, T.; Nazar, L. Spherical ordered mesoporous carbon nanoparticles with high porosity for lithium−sulfur batteries. *Angew. Chem., Int. Ed.* **2012**, *51*, 3591−3595.

(18) Jayaprakash, N.; Shen, J.; Moganty, S.; Corona, A.; Archer, L. Porous hollow carbon-sulfur composites for high-power lithium−sulfur batteries. *Angew. Chem., Int. Ed.* **2011**, *50*, 5904−5908.
(19) Gorkovenko, A.; Skotheim, T. A.; Xu, Z.-S.; Boguslavsky, L. I.; Deng, Z.; Mukherjee, S. P. U.S. Patent US6210831, April 3, 2001.
(20) Song, M.-S.; Han, S.-C.; Kim, H.-S.; Kim, J.-H.; Kim, K.-T.; Kang, Y.-M.; Ahn, H.-J.; Dou, S. X.; Lee, J.-Y. Effects of nanosized adsorbing material on electrochemical properties of sulfur cathodes for Li/S secondary batteries. *J. Electrochem. Soc.* **2004**, *151*, A791−A795.
(21) Choi, Y. J.; Jung, B. S.; Lee, D. J.; Kim, K. W.; Ahn, H. J.; Cho, K. K.; Gu, H. B. Electrochemical properties of sulfur electrode containing nano Al_2O_3 for lithium/sulfur cell. *Phys. Scr.* **2007**, *T129*, 62−65.
(22) Zhang, Y. G.; Zhao, Y.; Yermukhambetova, A.; Bakenov, Z.; Chen, P. Ternary sulfur/polyacrylonitrile/$Mg_{0.6}Ni_{0.4}O$ composite cathodes for high performance lithium/sulfur batteries. *J. Mater. Chem. A* **2013**, *1*, 295−301.
(23) Ji, X.; Evers, S.; Black, R.; Nazar, L. F. Stabilizing lithium−sulphur cathodes using polysulphide reservoirs. *Nat. Commun.* **2011**, *2*, 325.
(24) Wei, S.; Zhang, H.; Huang, Y.; Wang, W.; Xia, Y.; Yu, Z. Pig bone derived hierarchical porous carbon and its enhanced cycling performance of lithium−sulfur batteries. *Energy Environ. Sci.* **2011**, *4*, 736−740.
(25) Evers, S.; Yim, T.; Nazar, L. F. Understanding the nature of absorption/adsorption in nanoporous polysulfide sorbents for the Li−S battery. *J. Phys. Chem. C* **2012**, *116*, 19653−19658.
(26) Chung, S.-H.; Manthiram. Carbonized eggshell membrane as a natural polysulfide reservoir for highly reversible Li−S batteries. *Adv. Mater.* **2014**, *26*, 1360−1365.
(27) Chung, S.-H.; Manthiram. A natural carbonized leaf as a polysulfide inhibitor for high-performance lithium-sulfur battery cells. *ChemSusChem* **2014**, *7*, 1655−1661.
(28) Brun, N.; Sakaushi, K.; Eckert, J.; Titirici, M. M. Carbohydrate-derived nanoarchitectures: On a synergistic effect toward an improved performance in lithium−sulfur batteries. *ACS Sustainable Chem. Eng.* **2014**, *2*, 126−129.
(29) Xu, Q.; Kong, Q.; Liu, Z.; Wang, X.; Liu, R.; Zhang, J.; Yue, L.; Duan, Y.; Cui, G. Cellulose/polysulfonamide composite membrane as a high performance lithium-ion battery separator. *ACS Sustainable Chem. Eng.* **2014**, *2*, 194−199.
(30) Li, Z.; Xu, Z.; Tan, X.; Wang, H.; Holt, C. M. B.; Stephenson, T.; Olsen, B. C.; Mitlin, D. Mesoporous nitrogen-rich carbons derived from protein for ultra-high capacity battery anodes and supercapacitors. *Energy Environ. Sci.* **2013**, *6*, 871−878.
(31) Sing, K. S. W.; Everett, D. H.; Haul, R. A. W.; Moscou, L.; Pierotti, R. A.; Rouquerol, J.; Siemieniewska, T. Reporting physisorption data for gas/solid systems with special reference to the determination of surface area and porosity. *Pure Appl. Chem.* **1985**, *57*, 603−619.
(32) Barchasz, C.; Molton, F.; Duboc, C.; Leprêtre, J.-C.; Patoux, S.; Alloin, F. Lithium/sulfur cell discharge mechanism: An original approach for intermediate species identification. *Anal. Chem.* **2012**, *84*, 3973−3980.
(33) Yamin, H.; Gorenshtein, A.; Penciner, J.; Sternberg, Y.; Peled, E. Lithium sulfur battery: Oxidation/reducstion mechanisms of polysulfides in THF solutions. *J. Electrochem. Soc.* **1988**, *135*, 1045−1048.
(34) Chung, S.-H. Manthiram, High-performance Li−S batteries with an ultra-lightweight MWCNT-coated separator. *J. Phys. Chem. Lett.* **2014**, *5*, 1978−1983.
(35) Jung, D. S.; Hwang, T. H.; Lee, J. H.; Koo, H. Y.; Shakoor, R. A.; Kahraman, R.; Jo, Y. N.; Park, M.-S.; Choi, J. W. Hierarchical porous carbon by ultrasonic spray pyrolysis yields stable cycling in lithium−sulfur battery. *Nano Lett.* **2014**, *14*, 4418−4425, DOI: 10.1021/nl501383g.
(36) Cheon, S. E.; Ko, K. S.; Cho, J. H.; Kim, S. W.; Chin, E. Y.; Kim, H. T. Rechargeable lithium sulfur battery. II. Rate capability and cycle characteristics. *J. Electrochem. Soc.* **2003**, *150*, A800−A805.